02

Crystal-field levels of Sm^{3+} ion in low-dimensional magnetic $Cu_3Sm(SeO_3)_2O_2Cl$

© S.A. Klimin[1], E.S. Kuznetsova[2], P.S. Berdonosov[2]

[1] Institute of Spectroscopy, Russian Academy of Sciences, 108840 Troitsk, Moscow, Russia
[2] Faculty of Chemistry, Lomonosov Moscow State University, 119991 Moscow, Russia

e-mail: klimin@isan.troitsk.ru

Received August 20, 2021
Revised August 20, 2021
Accepted September 03, 2021

The transmission spectra of a two-dimensional frustrated magnetic $Cu_3Sm(SeO_3)_2O_2Cl$ were measured in the region of $f-f$-transitions of the Sm^{3+} ion in a wide temperature range (4–300 K). The energies of 40 crystal-field levels of the Sm^{3+} ion are determined for the ground and excited multiplets in the spectral region of 2000–10 000 cm^{-1}. The spectra revealed two magnetic phase transitions: at temperature of $T_N = 35$ K, magnetic ordering occurs, and at temperature of $T_R = 8.5$ K — spin-reorientation transition. The ground Kramers doublet of the Sm^{3+} ion splits only at a low-temperature phase transition. The data obtained on the energy states of the ground multiplet $^6H_{5/2}$ of the Sm^{3+} ion are used to calculate the contribution of samarium to the heat capacity of $Cu_3Sm(SeO_3)_2O_2Cl$.

Keywords: francisite-like phases with rare-earth elements, optical spectroscopy, Kramers doublets, magnetic phase transitions, spin reorientation.

DOI: 10.21883/EOS.2022.01.52985.37-21

Introduction

The magnetic properties of the compound $Cu_3Sm(SeO_3)_2O_2Cl$ are determined by the interaction of two magnetic subsystems: the two-dimensional d-subsystem of copper ions Cu^{2+} and f-subsystem of samarium ions Sm^{3+}. The study of the properties of crystals with mixed f- and d-magnetic subsystems is one of the areas of study carried out in the Fourier spectroscopy laboratory of the Institute of Spectroscopy of the Russian Academy of Sciences under the guidance of Professor Marina Nikolaevna Popova, this volume of journal „Optics and Spectroscopy“ deals with her jubilee. In M.N. Popova works using high-resolution Fourier spectroscopy in crystals containing f- and d-elements new effects of the interaction of various subsystems [1–3] were discovered, the importance of studies of the spectra of $f-f$-transitions was specified, since, in combination with calculation methods within the framework of the crystal field theory, such studies provide important information, including on the magnetic properties of a crystal [4,5], the practical value of spectroscopic data was justified, in particular, for calculating and explaining anomalies in thermodynamic characteristics [6–8], as well as for determining the type of magnetic structure [9,10], important conclusions were made about the hierarchy of magnetic interactions in these systems [11–13], which are used in the analysis of the data obtained in this work. In particular, it is important that the magnetic $d-d$-interactions are predominant, and in most cases they are responsible for the magnetic ordering. In this case, f-subsystem is magnetized in the internal field created by the ordered d-subsystem. In its turn, it is f-subsystem, which in most cases consists of strongly anisotropic ions, that can impose one or another type of magnetic structure and be the cause of spin-reorientation transitions.

The compound $Cu_3Sm(SeO_3)_2O_2Cl$ is a structural analogue of the francisite mineral $Cu_3Bi(SeO_3)_2O_2Cl$ [14] synthesized in laboratory conditions. This mineral was recently discovered [15] and named after Glen Francis, who first drew attention to small apple-green crystals. The crystal structure of francisite allows the replacement of some elements with chemically related ones ($Se \rightarrow Te$, $Cl \rightarrow Br, I$) [16,17]. In the paper [18] the fundamental possibility of replacing bismuth with a rare-earth element (REE), namely, with Er^{3+}, was demonstrated for the first time, and the resulting compound turned out to be isostructural to the original francisite. Subsequently, using methods of artificial synthesis of crystals, analogs of francisite with REE [14,19] were obtained, which are of interest for studying systematic features in a series of isostructural compounds [20].

The crystal structure of the mineral $Cu_3Bi(SeO_3)_2O_2Cl$ was determined in the papers [15,21,22]. It was shown that it crystallizes in the space group $Pmmn$. The main distinguishing feature of the structure is the two-dimensional nature of the copper sublattice (Fig. 1). As for samarium, it is located in the bismuth position with C_{2v} symmetry, in which the crystal field splits the multiplets $^{2S+1}L_J$ of the samarium ion Sm^{3+} into $J + 1/2$ Kramers doublets. Studies of francisite and its analogues have revealed their interesting magnetic properties and have made it possible

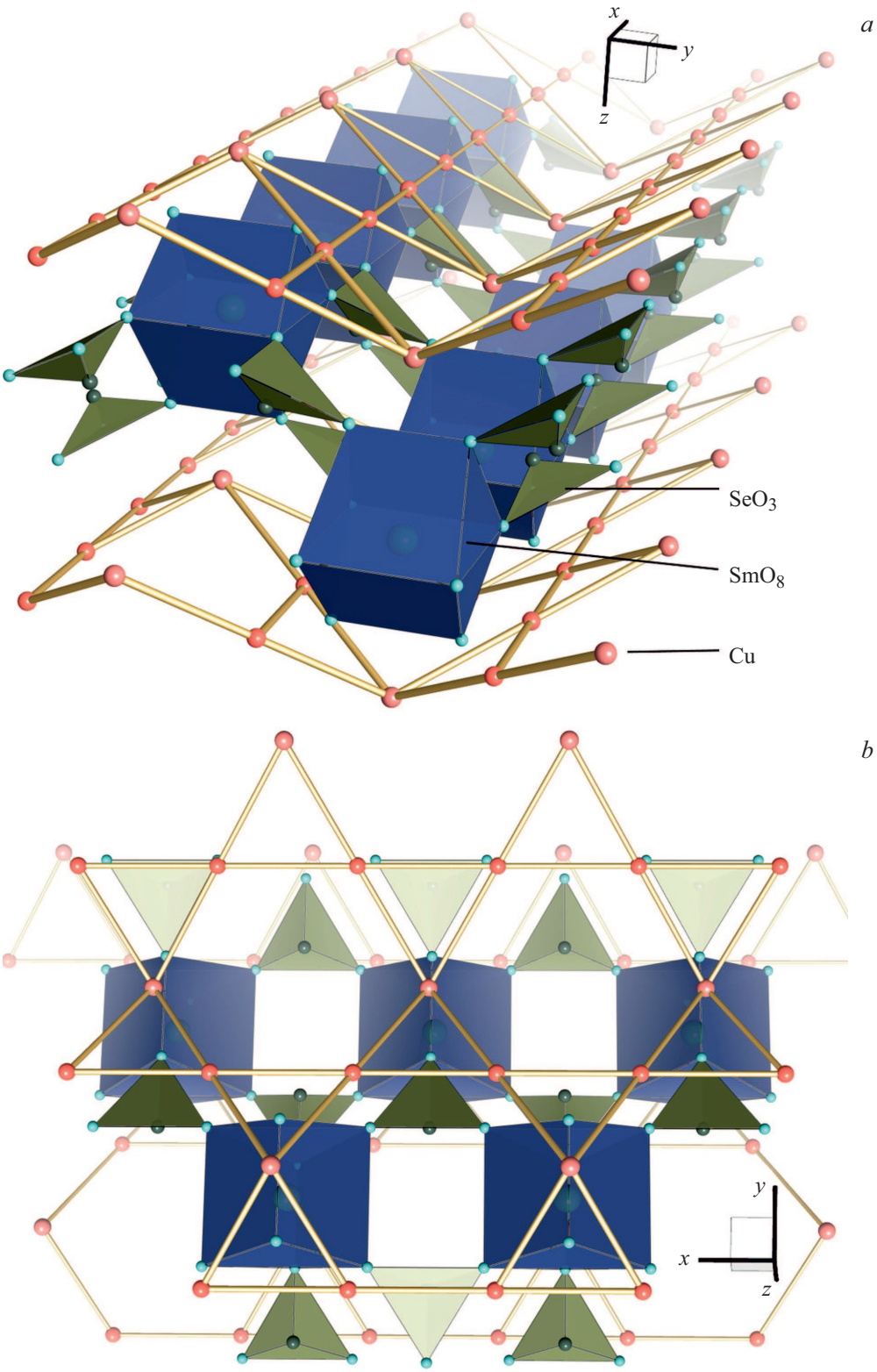

Figure 1. Crystal structure of $Cu_3Sm(SeO_3)_2O_2Cl$. Two copper planes connected by SmO_8 polyhedrons (*a*). Copper plane with Kagome type lattice (*b*).

to classify these compounds as two-dimensional frustrated magnetics. The magnetic properties of the bromine analogue of francisite $Cu_3Bi(SeO_3)_2O_2Br$ have been studied in most detail. According to the paper [23], in this crystal, Cu–Cu exchange magnetic interactions inside the layers are by more than two orders of magnitude higher than

the interlayer ones, which leads to a low temperature of magnetic ordering of the bromine analogue of francisite, $T_N = 27.4$ K. For analogues of francisite with REE, Neel temperatures are slightly higher and are in the range of 34–38 K [24–33].

The samarium analogue of francisite was previously studied in the paper [27] using magnetic, thermodynamic, optical, and theoretical methods. In addition to the phase transition with antiferromagnetic (AFM) ordering at temperature of $T_N = 35$ K, which is characteristic for the entire series of rare-earth analogues of francisite, a spin-reorientation transition was also found in it at temperature of $T_R = 8.5$ K. Namely optical spectroscopy made it possible to draw a conclusion about the nature of the low-temperature transition. This conclusion, based on the M.N. Popova papers, follows from the specific temperature behavior of the splitting of the ground Kramers doublet of the Sm^{3+} ion, obtained from data of the optical spectroscopy of $f-f$-transitions in the samarium ion. Despite the magnetic ordering that is established in the copper subsystem below the temperature of $T_N = 35$ K, and the appearance of an effective magnetic field created by the ordered copper subsystem in the position of the rare-earth ion, the ground Kramers doublet of the Sm^{3+} ion does not split until the spin-reorientation temperature of $T_R = 8.5$ K, below which this doublet splits. This behavior is associated with the specifics of the magnetic anisotropic properties of d- and f-subsystems. The splitting of the Kramers doublet Δ_0 can be described by the quasi-Zeeman formula

$$\Delta_0 = \mu_B \sqrt{\sum_{i=x,y,z} (g_i^{Sm} B_{ef,i}^{Cu})^2}, \quad (1)$$

where μ_B is Bohr magneton, g_i^{Sm} $(i = x, y, z)$ are magnetic g-factors of samarium, $B_{ef,i}^{Cu}$ $(i = x, y, z)$ are components of effective (exchange) magnetic field generated by ordered magnetic subsystem of copper in position of samarium. Considering relation (1), it is easy to explain the temperature behavior of Δ_0 in the case of the samarium ion in $Cu_3Sm(SeO_3)_2O_2Cl$. Let us assume that the magnetic g-factor of samarium, determined by the crystal field, is strongly anisotropic (one or two of its components are equal to zero). Then, the absence of splitting Δ_0 in the temperature range $T_N > T > T_R$ is due to the fact that the effective field B_{ef}^{Cu} has such direction that the corresponding component of the magnetic g-factor of samarium, and hence Δ_0, are equal to zero. At temperature of T_R, the copper magnetic moments are reoriented, and the effective field rotates along the coordinate for which the component g_i^{Sm} is maximum, resulting in splitting of the ground samarium doublet. The reason for the rotation is the energy gain of the crystal due to the excess of the energy decreasing of the ground state of the RE ion over the energy required for the spins flip of the copper ions. Literature does not contain information on the magnetic properties of the three-charged samarium ion in $Cu_3Sm(SeO_3)_2O_2Cl$. The magnetic g-factor of samarium can be calculated within the framework of the crystal field theory. To carry out such calculation, one needs the energy values of the crystal-field levels of the samarium ion in $Cu_3Sm(SeO_3)_2O_2Cl$, which are not available in the literature.

In this paper we present data on the energy structure of the crystal-field levels of the Sm^{3+} ion in the $Cu_3Sm(SeO_3)_2O_2Cl$ structure, and phase transitions in this compound are discussed.

Experiment

Polycrystalline samples of $Cu_3Sm(SeO_3)_2O_2Cl$ were obtained by solid-phase synthesis at the Faculty of Chemistry of Lomonosov Moscow State University. The synthesis is described in detail in the papers [14,19,33]. The results of the X-ray study showed that the sample has a structure with space group $Pmmn$ and does not contain other phases. To study the transmission spectra, we used the standard method for preparing tablets filled with potassium bromide. The polycrystalline powder $Cu_3Sm(SeO_3)_2O_2Cl$ was carefully ground in an agate pounder in amount of ~ 12 mg, then was mixed with ~ 300 mg of optically pure KBr. Further, the resulting mixture was pressed into a tablet with a diameter of 13 mm at a pressure of ~ 6 atm.

The transmission spectra were measured on Bruker IFS 125HR high-resolution Fourier spectrometer. To cool the sample to low temperatures a CryoMech ST403 closed-cycle optical helium cryostat with two-stage cooling was used. To pump the internal circuit of the cryostat to residual vacuum better than $5 \cdot 10^{-4}$ Torr, VarianV70 Turbo turbomolecular pump was used. The sample is cooled by thermal contact with a holder made of copper. To improve heat transfer, the sample was wrapped in indium foil. Temperature measurement and control of the cooling process were carried out using two diode silicon sensors. The temperature mode was controlled using a Scientific Instruments 9700 two-channel thermal controller.

Experimental results and discussion

The transmission spectrum of sample $Cu_3Sm(SeO_3)_2O_2Cl$ in spectral range of 3500–10 000 cm^{-1} is shown in Fig. 2. The spectrum shows narrow absorption lines grouped into multiplets. They are due to $f-f$-transitions in the Sm^{3+} ion. Comparison with the Dieke [34] diagram ensures easy identification of the multiplets. Besides, one more feature of the spectrum is noticeable: as the wavenumber increases, the intensity of the transmitted light constantly decreases. This is due to the fact that light scattering occurs in the sample, and it is the higher, the higher the frequency of the incident radiation is.

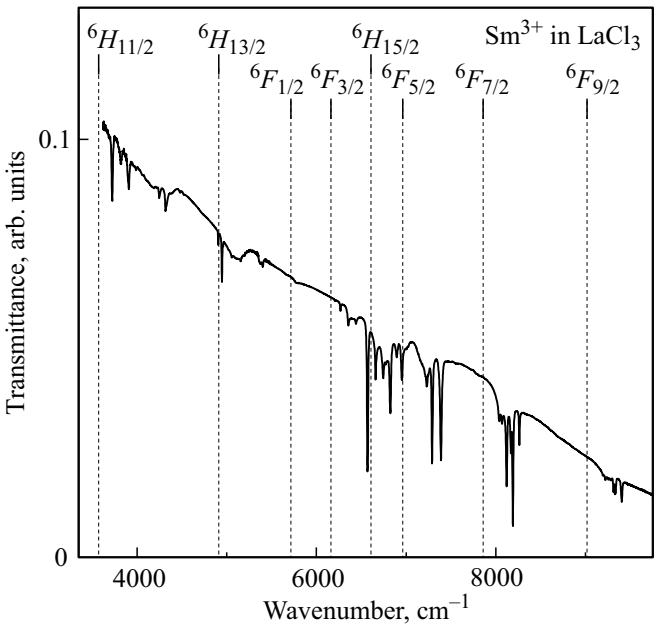

Figure 2. General view of transmission spectrum of $Cu_3Sm(SeO_3)_2O_2Cl$ in spectral range of $3500-10\,000\,cm^{-1}$. The temperature is 150 K. Above positions of Sm^{3+} multiplets in $LaCl_3$ are shown according to Dieke [34].

Crystal-field levels of the Sm^{3+} ion in $Cu_3Sm(SeO_3)_2O_2Cl$

In order to determine the energies of the crystal-field levels of the Sm^{3+} ion, we examined the low-temperature transmission spectra, using advantage of both the spectral lines narrowing and the fact that at low temperatures only the ground Kramers doublet of samarium is populated, which reduces the number of lines observed in the spectrum. Figure 3 shows the experimental spectra in the region of $^6H_{9/2}$ multiplet. The „raw" transmission spectrum shown in Fig. 3, *a* contains not only absorption lines of samarium, but also many spectral features not related to $f-f$-transitions, and associated with (i) spectral path including optical elements and detector, (ii) light scattering and the quality of both the tablet and the potassium bromide used for pressing, which is characterized by high hygroscopicity, and (iii) „extra" absorption lines, which can be due to residual gases in the optical path (mainly water vapor), combined multiphonon processes, and the possible presence of a small amount of impurity phases unregistered by X-ray. The „normalized" spectrum (Fig. 3, *b*) was obtained by dividing the „raw" spectrum by the empirical baseline. „Extra" lines mentioned above are marked with asterisks.

In order to get rid of all unwanted spectral bands not associated with $f-f$-transitions and to determine the energies of the crystal-field levels, we used the specific features of the behavior of spectral lines upon temperature change. As was shown in the paper [27], in $Cu_3Sm(SeO_3)_2O_2Cl$ the spin-reorientation transition occurs at temperature of $T_R = 8.5$ K. In a narrow temperature range, splitting of the ground Kramers doublet occurs, and as a result, the spectral lines are shifted to the high-frequency side by, on average, half of the splitting value Δ_0. If we take the ratio of two „raw" transmission spectra, one of which was measured at a temperature slightly higher T_R, and the other — at slightly lower temperature, then the resulting spectrum will contain only lines of $f-f$-transitions. Moreover, each line will participate twice: the line from the spectrum-numerator will look like an absorption line, and the shifted line from the spectrum-denominator will look like an emission line.

An example of such division is shown in Fig. 3, *c* for the spectrum in the region of the $^6H_{9/2}$ multiplet. In this case, the spectrum measured at 11 K was divided by the spectrum at 7 K. The presented multiplet consists of five levels (Kramers doublets, the number of which is equal to $(2J+1)/2$, where J is the total moment for this multiplet). Exactly five resonances are observed in the obtained spectrum, and all „ex-

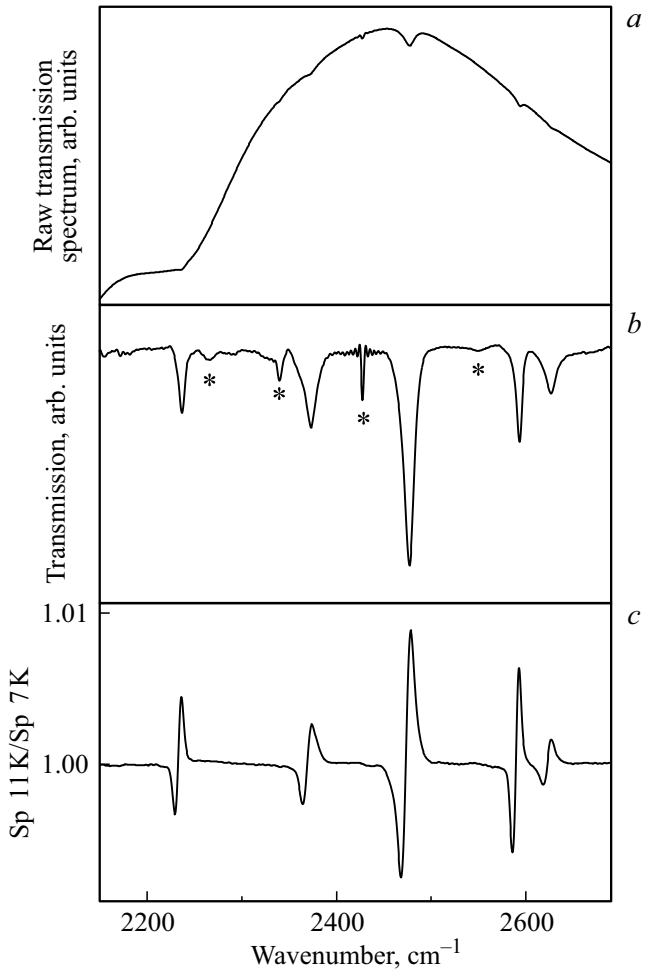

Figure 3. Spectra in region of multiplet $^6H_{9/2}$: „raw" transmission spectrum at temperature of 7 K (*a*), „normalized" transmission spectrum at 7 K (*b*), „differentiated" spectrum obtained by dividing „raw" spectra measured at temperatures of 11 K/7 K (*c*). Asterisks denote „extra" lines of different nature (see text).

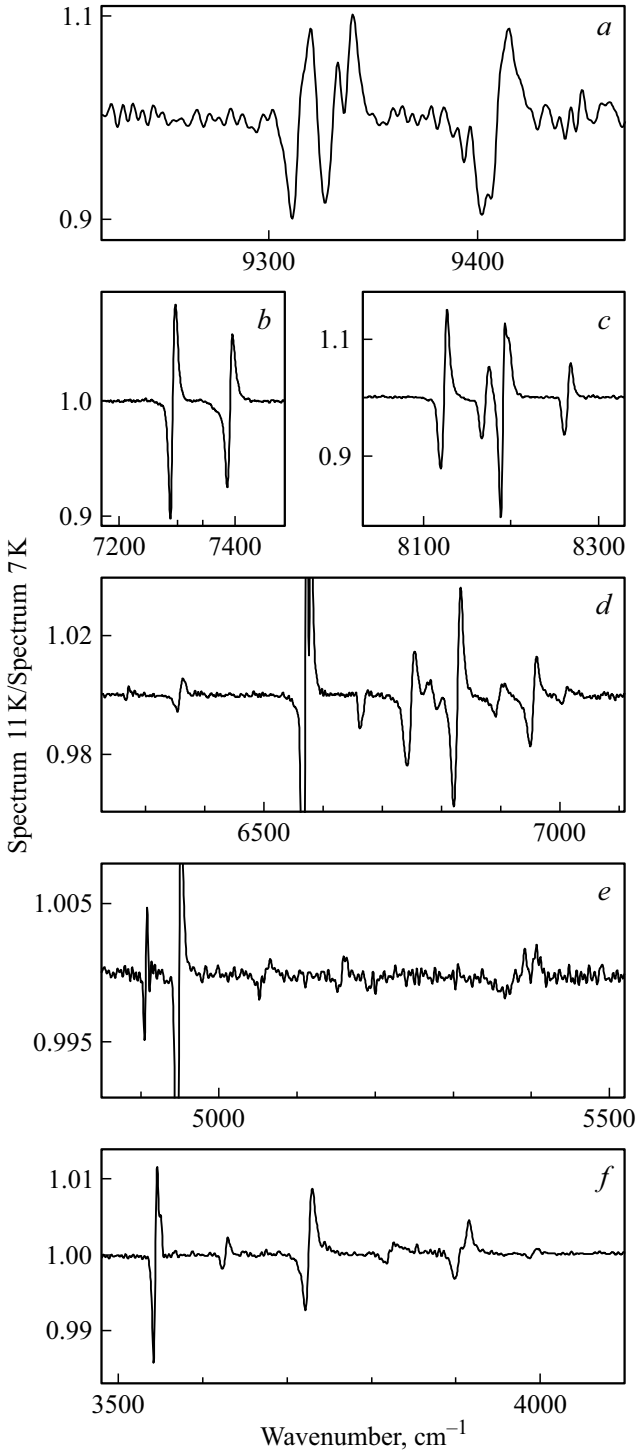

Figure 4. „Differentiated" spectra for multiplets ${}^6F_{9/2}$ (a), ${}^6F_{5/2}$ (b), ${}^6F_{7/2}$ (c), ${}^6F_{3/2}+{}^6H_{15/2}$ (d), ${}^6H_{13/2}$ (e), ${}^6H_{11/2}$ (f) of ion Sm^{3+} in $Cu_3Sm(SeO_3)_2O_2Cl$.

tra" lines turned out to be compensated. The minima of the „absorption" lines in this spectrum correspond to the energies of the crystal-field levels of the Sm^{3+} ion for a temperature of 11 K. Figure 4 shows similar „differential" spectra for multiplets ${}^6F_{9/2}$, ${}^6F_{7/2}$, ${}^6F_{5/2}$, ${}^6F_{3/2}+{}^6H_{15/2}$, ${}^6H_{13/2}$, ${}^6H_{11/2}$, from which we could define energies of crystal-field levels of the Sm^{3+} ion for specified multiplets. The Table contains all found energies.

Energy structure of the ground multiplet ${}^6H_{5/2}$ of the Sm^{3+} ion in $Cu_3Sm(SeO_3)_2O_2Cl$ — structural analogue of francisite

To determine the energy structure of the ground multiplet ${}^6H_{5/2}$, we studied the spectra at an elevated temperature, when two excited levels of this multiplet become populated, and, accordingly, lines associated with transitions originating from these levels appear in the spectrum. The transmission spectra at various temperatures for three multiplets are shown in Fig. 5. The main lines decrease in intensity with temperature increasing due to decreased population of the ground state. At the same time, lines corresponding to transitions from excited levels of the ground multiplet appear in the spectrum, and their intensity increases. These appearing lines are shifted to the low frequency region with respect to the main lines in accordance with the energy gap between the ground state and the excited ones. The shifts correspond to the energies of the crystal-field levels of the ground multiplet (levels II and III in the diagram to Fig. 5, a) and equal to 115 cm^{-1} for level II and 270 cm^{-1} for level III. These data are also included in the Table.

The resulting energy diagram of the crystal-field states of the Sm^{3+} ion is important for further studies. These data are necessary for carrying out calculation within the framework of the crystal field theory. In particular, the spectroscopic data of the study of $f-f$-transitions clearly indicate a mismatch between the magnetic anisotropy of the f- and d-subsystems and the main role of the magnetic properties of the Sm^{3+} ion in the realization of spin-reorientation transition. The calculation will give a quantitative estimate of the single-ion anisotropy of samarium, which has not yet been studied so far.

Magnetic phase transitions in $Cu_3Sm(SeO_3)_2O_2Cl$

The absorption spectra for different multiplets were measured in detail over a wide temperature range. To visualize the representation of the temperature dependences of the transmission spectra, shown in Fig. 6, together with the splitting diagram of Kramers doublets in different magnetic phase states, the color intensity maps were constructed with the frequency-temperature scale for two selected multiplets. The Figure for each multiplet is arranged as follows: in the upper half there are several spectral contours in this region, for each sample temperature is marked with its own color, and in the lower part there is a color map in the temperature–wavenumber axes, where the color indicates the intensity (color scale from black to orange).

The most obvious feature in the temperature behavior of the spectral lines, as can be seen in Fig. 6, is observed

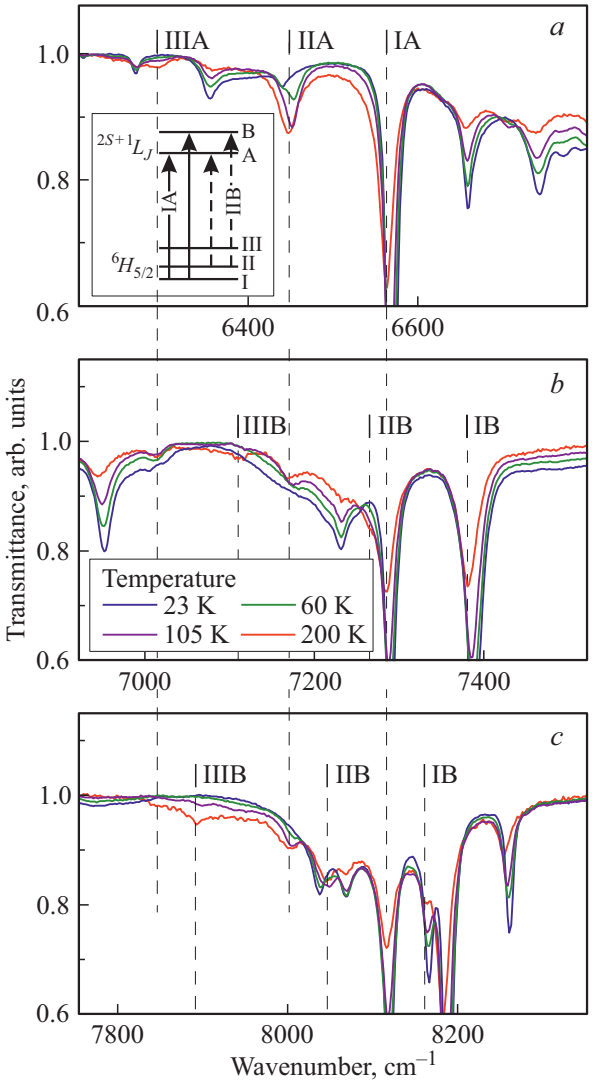

Figure 5. Absorption spectra in region of multiplets $^6F_{3/2} + {}^6H_{15/2}$ (a), $^6F_{5/2}$ (b) and $^6F_{7/2}$ (c) of the Sm^{3+} ion in $Cu_3Sm(SeO_3)_2O_2Cl$ at various temperatures. The insert (a) explains the designation of transitions and their corresponding spectral lines. Insert (b) — legend of temperature.

at the temperature ~ 8.5 K: all lines are shifted, for some lines splitting is noticeable, for example, for line 8231 cm^{-1} in Fig. 6, *d, e*, at that the high-frequency component of the line „freezes out“ very quickly, i.e. its intensity quickly drops with temperature decreasing. This behavior unambiguously indicates the splitting of the ground Kramers doublet at temperatures below $T_R \approx 8.5$ K, as shown in the diagram in Fig. 6, *a* for AFM2 phase ($T < T_R$). Above the temperature T_R no signs of splitting of the ground Kramers doublet of the Sm^{3+} ion were found, since almost all the lines (with the only exception of the line 6566 cm^{-1}) do not experience splitting. The occurrence of splitting of the Kramers doublet (in this case, we are talking about the ground doublet) can only be due to the influence of the magnetic field, in this case, the internal field. Thus, at a temperature near 8.5 K a magnetic phase transition takes place, which is in agreement with the data of the paper [27], according to which this transition is a spin-reorientation one.

Another feature in the spectra is observed at the temperature of $T_N = 35$ K. In the paper [27] it was shown that below the temperature of T_N the only one of the registered lines, i.e. the line 6566 cm^{-1}, splits. This is also clearly seen in the spectra presented in this paper (insert to Fig. 6, *b*). This line splitting at temperature above $T_R \approx 8.5$ K is related to the upper level (Kramers doublet) splitting of the spectral transition, as shown on the right side of the levels diagram for the phase AFM 1 (Fig. 6, *a*). The splitting of the line 6566 cm^{-1} unambiguously indicates the presence of a magnetically ordered state at temperatures above $T_R \approx 8.5$ K. However, it is difficult to determine the phase transition temperature from this line splitting due to the rather large inhomogeneous width of the spectral lines. On the intensity maps in Fig. 6, *c, e* one can see that near the temperature of $T_N = 35$ K the color of some lines becomes brighter due to the peak intensity increasing of these lines, which is also seen if we compare the absorption lines (for example, 8119 and 8188 cm^{-1}) in the spectra measured at temperatures of 44 and 12 K (above and below magnetic ordering temperatures, respectively). Such the peak intensity increasing is associated with the half-width decreasing of the spectral lines. The narrowing of the spectral lines with temperature decreasing below 35 K is most pronounced for lines that do not have splitting of the upper level of the spectral transition, as shown on the left side of the levels diagram for the phase AFM 1 (Fig. 6, *a*). For some of these lines, namely the lines 2230, 7386, and 8262 cm^{-1}, Fig. 7 shows half-widths vs. temperature diagrams. At temperatures below 35 K, all three spectral lines experience a significant narrowing. It is natural to associate such a narrowing with the decreasing of contribution to the broadening associated with magnetic disorder. Thus, from the dependences presented we were able to determine the magnetic ordering temperature $T_N = 35 \pm 1$ K (in accordance with the paper [27], in which the transition to the antiferromagnetic state was determined).

It is interesting, that the line half-widths increase in the vicinity of the low-temperature phase transition at the temperature of $T_R \approx 8.5$ K. The half-width increasing can be explained by the instability increasing of the magnetic structure upon cooling of the compound under study and approaching T_R. The system then undergoes spin-reorientation transition, and the instability rapidly disappears upon further cooling.

Thus, in the studied magnetic $Cu_3Sm(SeO_3)_2O_2Cl$, the features of low-temperature magnetism arise due to the competition between the anisotropies of two magnetic subsystems — copper and samarium. The magnetic ordering that occurs at the temperature of $T_N = 35$ K is realized due to the strongest magnetic $d-d$-interaction inside the copper subsystem. The resulting internal magnetic field magnetizes the samarium subsystem. The strong single-ion anisotropy

Crystal-field levels of the Sm^{3+} ion in $Cu_3Sm(SeO_3)_2O_2Cl$ at temperature of 11 K

Multiplet	Number of levels $(2J+1)$	Energies of crystal-field levels, cm^{-1}
$^6H_{5/2}$	3	0, 115*, 270*
$^6H_{9/2}$	5	2229.5, 2364.4, 2468, 2586, 2618.3
$^6H_{11/2}$	6	3541.7, 3623.3, 3721.6, 3817, 3899, 3987
$^6H_{13/2}$	7	4904, 4946, 5052, 5153, 5368, 5400
$^6F_{1/2}$	1	–
$^6F_{3/2}$	2	6266, 6353.5
$^6H_{15/2}$	8	6566, 6666, 6742, 6770, 6820, 6892, 6951, 7004
$^6F_{5/2}$	3	7288, 7386
$^6F_{7/2}$	4	8119, 8167, 8188, 8261
$^6F_{9/2}$	5	9311, 9327, 9403

Note. * At temperature 150 K.

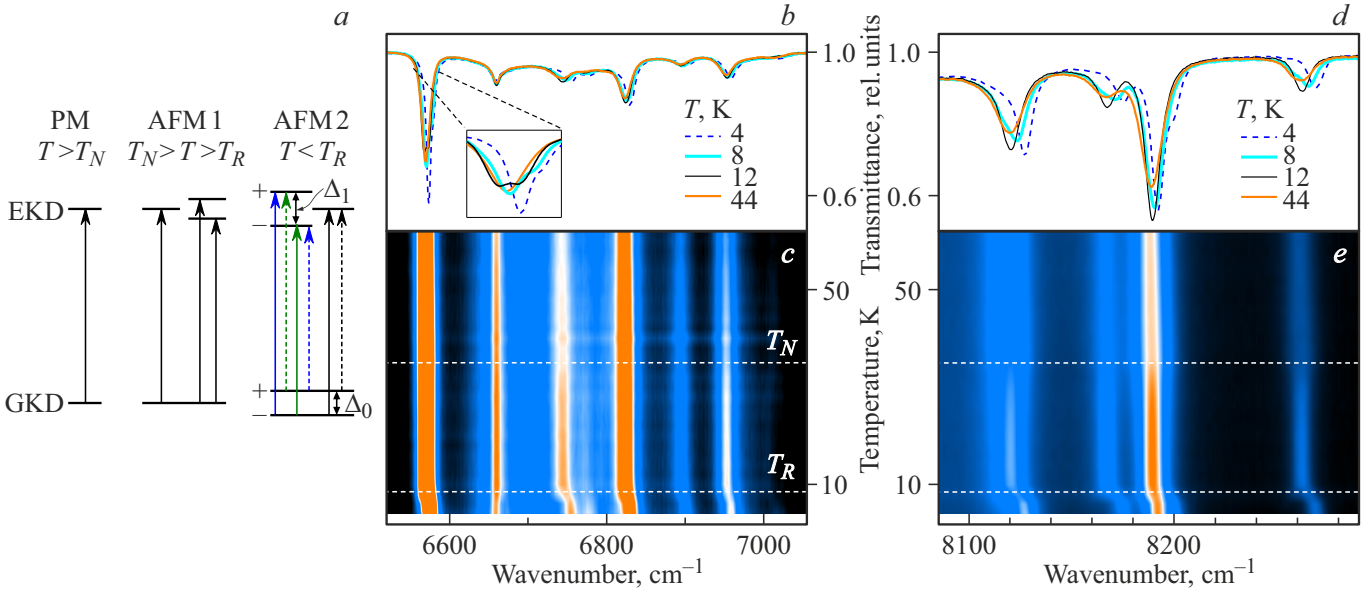

Figure 6. Diagram of ground and excited Kramers doublets (GKD and EKD, respectively) in various magnetic states (paramagnetic PM and antiferromagnetic AFM 1 and AFM 2) (a) and temperature dependencies for intermultiplet transitions $^6H_{5/2} \rightarrow {}^6H_{15/2}$ (b, c) and $^6H_{5/2} \rightarrow {}^6F_{7/2}$ (d, e) in ion Sm^{3+} in $Cu_3Sm(SeO_3)_2O_2Cl$ represented in form of transmission spectra at various temperatures (b, d) and intensity maps in coordinates temperature-wavenumber (c, e).

of samarium with the internal magnetic field increasing during sample cooling leads to instability of the magnetic structure and, finally, to spin reorientation.

Contribution of crystal-field levels of the Sm^{3+} ion to the heat capacity $Cu_3Sm(SeO_3)_2O_2Cl$

Using the data obtained in the experiment on the spectrum of energy states of the rare-earth ion, its contribution to the thermodynamic characteristics can be calculated. Such calculation helps to reveal the nature of the low-temperature features in the heat capacity $C(T)$ and the magnetic susceptibility $\chi(T)$ of REE-containing compounds. In particular, splitting $\Delta_0(T)$ of the ground doublet of Kramers ions is the cause of the Schottky anomalies. In the case of the investigated compound $Cu_3Sm(SeO_3)_2O_2Cl$, the contribution of samarium due to the dependence $\Delta_0(T)$ has already been calculated in the paper [27]. In the present work, using additionally obtained data on the energies of the other two excited crystal-field levels of the ground multiplet $^6H_{5/2}$, we were also able to calculate the contribution of these states to the heat capacity. To do this, we used the

following relation, obtained in the paper [35]:

$$C_{\mathrm{Sm}}(T) = R \sum_{\substack{i,j=1 \\ j<i}}^{N} \left(\frac{E_i - E_j}{kT} \right)^2 n_i n_j, \qquad (2)$$

where R is universal gas constant, k is Boltzmann constant, E_i and E_j are energies, n_i and n_j are populations of ith and jth states, N is the total number of states involved in the calculation. The populations comply with the Boltzmann distribution:

$$n_i = \frac{e^{-\frac{E_i}{kT}}}{\sum\limits_{j=1,N} e^{-\frac{E_j}{kT}}}, \qquad (3)$$

For calculation we used a set of six states (three Kramers doublets of ground multiplet $^6H_{5/2}$ of the Sm^{3+} ion), and namely $E_1 = 0\,\mathrm{cm}^{-1}$, $E_2 = \Delta_0(T)$, $E_3 = E_4 = 115\,\mathrm{cm}^{-1}$, $E_5 = E_6 = 270\,\mathrm{cm}^{-1}$. Function $\Delta_0(T)$ was prepared from the analysis of the temperature behavior of all spectral lines. In particular, we used lines splitting into four components (see, for example, lines 6566 and $8188\,\mathrm{cm}^{-1}$ in Figs. 6, *b* and 6, *d*, respectively). Indeed, the spectra at temperature of 4 K exhibit two components corresponding to the transitions indicated by solid arrows on the left side of the levels diagram for phase AFM 2 (Fig. 6, *a*). The lines corresponding to the transitions indicated by the dashed arrows quickly freeze out due to the depletion of the population of the upper component of the split ground Kramers doublet. Therefore, to calculate Δ_0 we used the shifts of the ground components, assuming that the splitting is „mirror symmetric". The resulting function $\Delta_0(T)$ is shown in the insert to Fig. 8.

As a slight digression, let us pay attention to the fact that the two components for the lines 6566 and $8188\,\mathrm{cm}^{-1}$ discussed above have different intensities. The question of substantiating the difference between the intensities of the components of split line was considered in the paper [35]. Briefly, the intensity of specific transitions is determined by the matrix elements. It appears that the matrix elements are equal for the pair of transitions between the states „++" and „−−", as well as for the pair „+−" and „−+" (see diagram in Fig. 6, *a*, on which these pairs of transitions are shown in different colors for clarity). For the transitions „−+" and „−−", corresponding to transitions from the lower component of the split ground Kramers doublet (nonfreezing lines), the ratio of the matrix elements is arbitrary, and this explains the difference in intensities observed for components of the split lines 6566 and $8188\,\mathrm{cm}^{-1}$. Moreover, this reasoning helps to explain the temperature behavior of the line $6666\,\mathrm{cm}^{-1}$, which behaves in a supposedly strange way: it shifts towards low frequencies, being the only one of all the measured lines. In this case, the splitting of the upper Kramers doublet involved in the transition exceeds the splitting of the ground doublet. Just such a case is shown on the left side of the levels diagram for phase AFM 2 (Fig. 6, *a*). The component

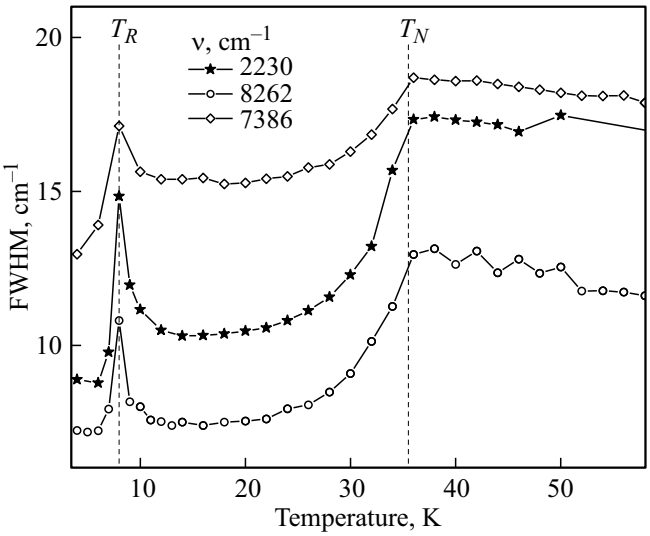

Figure 7. Full width at half-maximum (FWHM) of spectral lines with energies 2230, 7386 and $8262\,\mathrm{cm}^{-1}$ vs temperature.

corresponding to the transition „−−"has a lower frequency than the unsplit line. The component corresponding to the transition „−+"apparently has a very low intensity due to the small size of the matrix element.

The result of calculation of the samarium contribution to the heat capacity is shown in Fig. 8. This contribution is clearly divided into two non-overlapping parts. The low-temperature part is related to the splitting of the ground Kramers doublet; it is limited in temperature due to the specifics of the function $\Delta_0(T)$, which practically equals to zero at temperatures above T_R. The second part of the contribution is associated with excited doublets 115 and $270\,\mathrm{cm}^{-1}$, and it becomes noticeable only when the level $115\,\mathrm{cm}^{-1}$ population begins. We were also able to estimate the samarium contribution to the magnetic entropy released during the spin-reorientation transition at temperature of T_R (insert to Fig. 8). Samarium contribution is approximately equal to $2.6\,\mathrm{J}\cdot\mathrm{mol}^{-1}\cdot\mathrm{K}^{-1}$, which is practically half of entropy $(5\,\mathrm{J}\cdot\mathrm{mol}^{-1}\cdot\mathrm{K}^{-1})$ obtained from experimental data of heat capacity study of $Cu_3Sm(SeO_3)_2O_2Cl$ [27].

Conclusions

The spectroscopic study of $Cu_3Sm(SeO_3)O_2Cl$, the samarium structural analogue of the francisite mineral, was carried out in a wide spectral $(2000-10\,000\,\mathrm{cm}^{-1})$ and temperature $(4-300\,\mathrm{K})$ ranges. The diagram of crystal-field levels of the Sm^{3+} ion in $Cu_3Sm(SeO_3)O_2Cl$ is determined for the ground and several excited multiplets. The energies of 40 crystal-field levels are found. The data obtained are necessary for carrying out calculations within the framework of the theory of the crystal field, for finding the wave functions, which will allow, in particular, the magnetic g-factors calculation, which are important for the magnetic

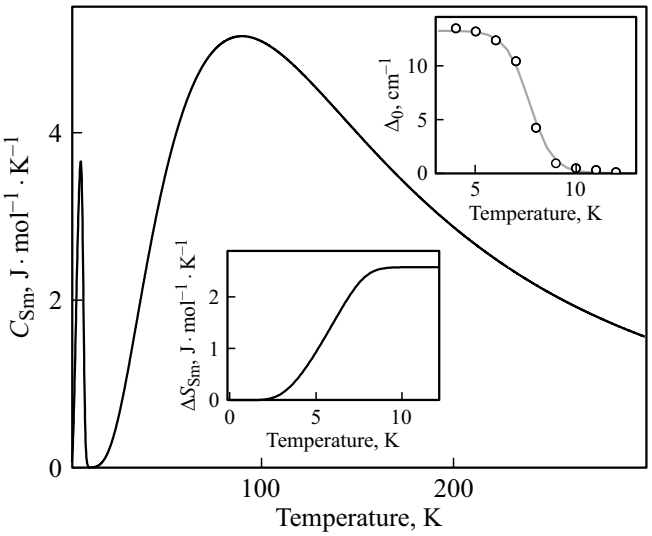

Figure 8. Calculated contribution of samarium C_{Sm} in heat capacity of $Cu_3Sm(SeO_3)_2O_2Cl$. The inserts show the temperature dependences of the splitting Δ_0 of the ground Kramers doublet of the Sm^{3+} ion and the magnetic entropy ΔS_{Sm} associated with samarium.

properties interpretation. Data on the energies of the ground multiplet are important for interpreting the thermodynamic characteristics.

The behavior of absorption lines at different temperatures was studied. The splitting of the Kramers doublets unambiguously indicates the presence of two phase transitions, in accordance with the previously published paper [27]. At the temperature of $T_N = 35$ K the ordering of the copper magnetic subsystem takes place. At a lower temperature of $T_R \approx 8.5$ K one more phase transition is observed.

The temperature behavior of the splitting of the ground Kramers doublet of samarium made it possible to make the conclusion about the nature of the low-temperature transition: it is a second-order spin-reorientation transition. The ground Kramers doublet of the Sm^{3+} ion splits only at temperatures below $T_R \approx 8.5$ K. The splitting absence in phase AFM in the temperature range $T_R < T < T_N$ can only be explained by the fact that the direction of the internal magnetic field acting on the samarium ion from the ordered copper subsystem coincides with the direction along which the magnetic g-factor of the ground state of samarium is minimum (has zero value). In the low-temperature phase AFM at $T < T_R$ the field turns toward the direction along which g-factor is maximum, and the ground samarium doublet splits. As a result, the energy of the ground state of the samarium ion decreases, and the system receives an energy gain. Thus, the significant anisotropy of samarium is the cause of the spin-reorientation transition.

Using spectroscopic data on the temperature dependences of the energies of the electronic states of the samarium ground multiplet, we were able to calculate the samarium contribution to the heat capacity.

Funding

The work of S.A.K. (spectroscopic studies) was carried out at Institute of Spectroscopy and supported by the Russian Foundation for Basic Research under the grant № 19-02-00251, the work of E.S.K. (synthesis of compounds) was carried out at Lomonosov Moscow State University and supported by the Russian Foundation for Basic Research under the grant № 19-33-60093 „Perspectivy“.

Conflict of interest

The authors declare that they have no conflict of interest.

References

[1] M.N. Popova, K.N Boldyrev. Phys. Usp., **62** (3), 275 (2019). DOI: 10.3367/UFNe.2018.06.038413
[2] M.N. Popova, T.N. Stanislavchuk, B.Z. Malkin, L.N. Bezmaternykh. Phys. Rev. Lett., **102** (18), 187403 (2009). DOI: https://doi.org/10.1103/PhysRevLett.102.187403
[3] S.A. Klimin, A.B. Kuzmenko, M.N. Popova, B.Z. Malkin, I.V. Telegina. Phys. Rev. B, **82** (17), 174425 (2010). DOI: 10.1088/1742-6596/1389/1/012039
[4] M.N. Popova, T.N. Stanislavchuk, B.Z. Malkin, L.N. Bezmaternykh. J. Phys.: Condens. Matter, **24**, 196002 (2012). DOI: https://doi.org/10.1088/0953-8984/24/19/196002
[5] M.N. Popova, S.A. Klimin, E.P. Chukalina, R.Z. Levitin, B.V. Mill, B.Z. Malkin, E. Antic-Fidancev. J. Alloys Compd., **380** (1–2), 84 (2004). DOI: https://doi.org/10.1016/j.jallcom.2004.03.032.
[6] M.M. Markina, B.V. Mill, G. Pristáš, M. Marcin, S.A. Klimin, K.N. Boldyrev, M.N. Popova. J. Alloys Compd. **779**, 380 (2019). DOI: https://doi.org/10.1016/j.jallcom.2018.11.227
[7] E.A. Popova, S.A. Klimin, M.N. Popova, R. Klingeler, N. Tristan, B. Büchner, A.N. Vasiliev. J. Magn. Magn. Mat., **331**, 133 (2013). DOI: https://doi.org/10.1016/j.jmmm.2012.11.019
[8] M.A. Kashchenko, S.A. Klimin, A.M. Balbashov, M.N. Popova. Phys. Stat. Solidi RRL, **10** (6), 462 (2016). DOI: 10.1002/pssr.201600076
[9] S.A. Klimin, A.S. Galkin, M.N. Popova. Phys. Lett. A. **376**, 1861 (2012), DOI: 10.1016/j.physleta.2012.03.013
[10] M.N Popova, S.A Klimin, R Troć, Z Bukowski. Solid State Commun., **102** (1), 71 (1997). DOI: https://doi.org/10.1016/S0038-1098(96)00700-4.
[11] M.N. Popova. J. Alloys Comp. **275–277**, 142 (1998). DOI: https://doi.org/10.1016/S0925-8388(98)00292-8.
[12] I.V. Paukov, M.N. Popova, B.V. Mill. Phys. Lett. A, **169** (4), 301 (1992). DOI: https://doi.org/10.1016/0375-9601(92)90463-V
[13] M.N. Popova, J. Magn. Magn. Mat., **321** (7), 716 (2009). DOI: https://doi.org/10.1016/j.jmmm.2008.11.033
[14] P.S. Berdonosov, V.A. Dolgikh. J. Inorg. Chem., **53** (9), 1353 (2008). DOI: 10.1134/S0036023608090027.
[15] A. Pring, B.M. Gatehouse, W.D. Birch. Amer. Miner., **75** (11–12), 1421 (1990).
[16] P. Millet, B. Bastide, V. Pashchenko, S. Gnatchenko, V. Gapon, Y. Ksari, A. Stepanov. J. Mater. Chem., **11** (4), 1152 (2001). DOI: 10.1039/b007920k
[17] R. Becker, M. Johnsson. Solid State Sci., **7** (4), 375 (2005). DOI: 10.1016/j.solidstatesciences.2004.10.045

[18] R. Berrigan, B.M. Gatehouse. Acta Crystallogr. C: Struct. Sci. Comm., **52**, 496 (1996). DOI: 10.1107/S0108270195014120
[19] P.S. Berdonosov, E.S. Kuznetsova, V.A. Dolgikh. Crystals, **8** (4), 159 (2018). DOI: 10.3390/cryst8040159
[20] N.N. Novikova, V.A. Yakovlev, E.S. Kuznetsova, P.S. Berdonosov, S.A. Klimin. Opt. Spectr., **130** (1), 49(2022), accepted
[21] S.V. Krivovichev, G.L. Starova, S.K. Filatov. Miner. Magazine, **63** (2), 263 (1999). DOI: 10.1180/minmag.1999.063.2.12.
[22] E.V. Nazarchuk, S.V. Krivovichev, O.Y. Pankratova, S.K. Filatov. Phys. Chem. Miner., **27**, 440 (2000). DOI: 10.1007/s002699900079
[23] M. Pregelj, O. Zaharko, A. Gunther, A. Loidl, V. Tsurkan, S. Guerrero. Phys. Rev. B., **86** (14), 144409 (2012). DOI: 10.1103/PhysRevB.86.144409
[24] K.V. Zakharov, E.A. Zvereva, P.S. Berdonosov, E.S. Kuznetsova, V.A. Dolgikh, L. Clark, C. Black, P. Lightfoot, W. Kockelmann, Z.V. Pchelkina, S.V. Streltsov, O.S. Volkova, A.N. Vasiliev. Phys. Rev. B, **90** (21), 214417 (2014). DOI: 10.1103/PhysRevB.90.214417
[25] M.M. Markina, K.V. Zakharov, E.A. Zvereva, R.S. Denisov, P.S. Berdonosov, V.A. Dolgikh, E.S. Kuznetsova, A.V. Olenev, A.N. Vasiliev. Phys. Chem. Minerals, **44** (4), 277 (2017). DOI: 10.1007/s00269-016-0855-0
[26] K.V. Zakharov, E.A. Zvereva, E.S. Kuznetsova, P.S. Berdonosov, V.A. Dolgikh, M.M. Markina, A.V. Olenev, A.A. Shakin, O.S. Volkova, A.N. Vasiliev. J. Alloys Compounds, **685**, 442 (2016). DOI: 10.1016/j.jallcom.2016.05.213
[27] K.V. Zakharov, E.A. Zvereva, M.M. Markina, M.I. Stratan, E.S. Kuznetsova, S.F. Dunaev, P.S. Berdonosov, V.A. Dolgikh, A.V. Olenev, S.A. Klimin, L.S. Mazaev, M.A. Kashchenko, M.A. Ahmed, A. Banerjee, S. Bandyopadhyay, A. Iqbal, B. Rahaman, T. Saha-Dasgupta, A.N. Vasiliev. Phys. Rev. B, **94** (5), 054401 (2016). DOI: 10.1103/PhysRevB.94.054401
[28] M.M. Markina, K.V. Zakharov, E.A. Ovchenkov, P.S. Berdonosov, V.A. Dolgikh, E.S. Kuznetsova, A.V. Olenev, S.A. Klimin, M.A. Kashchenko, I.V. Budkin, I.V. Yatsyk, A.A. Demidov, E.A. Zvereva, A.N. Vasiliev. Phys. Rev. B, **96** (13), 134422 (2017). DOI: 10.1103/PhysRevB.96.134422
[29] S.A. Klimin, I.V. Budkin. EPJ Web of Conferences, **132**, 02010 (2017). DOI: 10.1051/epjconf/201713202010
[30] M.M. Markina, P.S. Berdonosov, V.A. Dolgikh, K.V. Zakharov, E.S. Kuznetsova, A.N. Vasil'ev. Phys. Usp., **64**, 344, (2021). DOI: 10.3367/UFNe.2020.05.038773
[31] S.A. Klimin, P.S. Berdonosov, E.S. Kuznetsova. Opt. Spectrosc., **129** (1), 47 (2021). DOI: 10.1134/S0030400X21010094
[32] M.M. Markina, K.V. Zakharov, P.S. Berdonosov, V.A. Dolgikh, E.S. Kuznetsova, S.A. Klimin, O.B. Yumashev, A.N. Vasiliev. J. Magn. Magn. Mat., **492**, 165721 (2019). DOI: https://doi.org/10.1016/j.jmmm.2019.165721
[33] S.A. Klimin, P.S. Berdonosov, E.S. Kuznetsova., Low Temperature Physics, **47**(12), (2021)]
[34] G.H. Dieke. Spectra and Energy Levels of Rare Earth Ions in Crystals (Inter Science, New York, 1969).
[35] S.A. Klimin, A.S. Galkin, M.N. Popova, J. Alloys Compd., **625**, 193 (2015). DOI: https://doi.org/10.1016/j.jallcom.2014.11.129